Electron-transfer Properties of a Series of Bimetallic Rhodium(I) and Iridium(I) Complexes†

James E. Anderson,*[a] Thomas P. Gregory,[a] Gemma Net[b] and J. Carlos Bayón*[b]
[a] *Department of Chemistry, Boston College, Chestnut Hill, MA 02167, USA*
[b] *Departament de Química, Universitat Autònoma de Barcelona, Bellaterra, 08193 Barcelona, Spain*

The electron-transfer properties of $[NBu_4][M_2(dcbmi)(CO)_4]$, $[NBu_4][M_2(dcbmi)(cod)_2]$, (M = Rh or Ir) and $[NBu_4][Rh_2(dcbmi)(CO)_2(PPh_3)_2]$ (H_3dcbmi = 2-methylimidazole-4,5-dicarboxylic acid, cod = cycloocta-1,5-diene) were determined by electrochemical, UV/VIS and infrared spectroelectrochemical, and synthetic investigations. Relatively easy oxidations, but no reduction processes, were observed in acetonitrile, methylene chloride or tetrahydrofuran. The effect of the solvent on the electron-transfer properties of these complexes is discussed and the spectroelectrochemical results establish the site of electron transfer. Surface effects are observed and for $[NBu_4][Ir_2(dcbmi)(CO)_4]$ the growth of a conducting film has been monitored by cyclic voltammetry. Partial oxidation of $[Ir_2(dcmbi)(CO)_4]^-$ results in formation of $[NR_4]_{0.5}[Ir_2(dcbmi)(CO)_4]$ (R = Bu or Pr). Isotropic conductivities, measured on pressed pellets at room temperature, were 8×10^{-5} ohm^{-1} cm^{-1} for R = Pr and 2×10^{-5} ohm^{-1} cm^{-1} for R = Bu. The synthesis of $[ttf][Rh_2(dcbmi)(CO)_4]$ (ttf = tetrathiofulvalene) and the mixed-valence species $[Rh_2(dcbmi)(CO)_4]$ is also reported; the former exhibits solid-state conductive properties, presumably due to the ttf cation.

The synthesis of a series of anionic iridium(I) complexes designed to exhibit solid-state conductive properties upon partial oxidation has been recently reported.[1–4] Some of these complexes and their corresponding rhodium analogues are dinuclear, d^8, planar species of the general form $[NBu_4][M_2L(CO)_4]$ where L is a bridging nitrogen heterocyclic ligand containing two carboxylic acid groups such that each metal coordinates with a nitrogen and an oxygen.[1–3] The connectivity of $[M_2(dcbmi)(CO)_4]^-$ is shown, where the bridging ligand (dcbmi) is the trianion of 2-methylimidazole-4,5-dicarboxylic acid.[2]

The X-ray crystal structure[3] of $[NBu_4][Ir_2(dcbmi)(CO)_4]$ demonstrates that the dinuclear anion is planar, except for the hydrogens on the methyl group. In the solid state two anions are paired through an inversion centre producing two Ir···Ir intermolecular distances of 3.36 Å. The next pair of anions is slipped in the stacking axis by exactly half the length of the anion and a single Ir···Ir molecular distance of 3.30 Å is observed. Thus, the packing of the complex anions can be described as a double-step stair. The holes among these stairs are appropriate to pack the bulky NBu_4^+ cations. The crystallographic results[3] suggest a straight stack of the dinuclear ions would be possible if either a smaller cation were used or a cation-deficient partially oxidized material was generated. In agreement, salts of $[Ir_2(dcbmi)(CO)_4]^-$ with smaller cations, such as K^+, exhibit dark colours and solid-state conductivities that suggest strong extended intermolecular interactions.[2] Unfortunately, the low solubilities of these salts have precluded structural analysis.

In addition to $[NBu_4][M_2(dcbmi)(CO)_4]$, the related complexes $[NBu_4][M_2(dcbmi)(cod)_2]$ and $[NBu_4][M_2(dcbmi)(CO)_2(PPh_3)_2]$, where cod is cycloocta-1,5-diene, have also been synthesised.[2] All of these complexes are dinuclear, d^8, metal species in which interaction between the metal atoms within a given molecule is also possible. A number of photochemical, photophysical, electrochemical and reactivity studies[5–14] have been performed on species with similar structural characteristics.

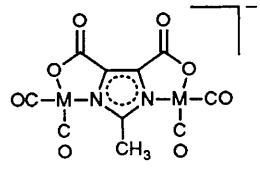

M = Rh^I or Ir^I

In this paper, we report the results from an electrochemical and spectroelectrochemical study of $[NBu_4][M_2(dcbmi)(CO)_4]$, $[NBu_4][M_2(dcbmi)(cod)_2]$ (M = Rh or Ir) and $[NBu_4][Rh_2(dcbmi)(CO)_2(PPh_3)_2]$. Nearly all of the compounds exhibit surface effects and for $[NBu_4][Ir_2(dcbmi)(CO)_4]$ growth of a conducting film on the electrode is monitored by cyclic voltammetry. In a manner similar to other $[Ir_2L(CO)_4]^-$ species,[1] partial oxidation of $[Ir_2(dcbmi)(CO)_4]^-$ results in formation of $[NR_4]_{0.5}[Ir_2(dcbmi)(CO)_4]$, where R = Bu or Pr. This formulation is based on elemental analysis and X-ray photoelectron spectroscopy (XPS). The synthesis and characterization of $[ttf][Rh_2(dcbmi)(CO)_4]$ {ttf = tetrathiofulvalene [2-(1,3-dithiol-2-ylidene)-1,3-dithiole]} and the mixed-valence rhodium(I,II) species $[Rh_2(dcbmi)(CO)_4]$ are also reported. Solid-state conduction data are presented for $[NBu_4]_{0.5}[Ir_2(dcbmi)(CO)_4]$, $[NPr_4]_{0.5}[Ir_2(dcbmi)(CO)_4]$ and $[ttf][Rh_2(dcbmi)(CO)_4]$. In the latter case, the conductive properties are primarily due to the ttf cation.[15,16]

The electrochemical data on these compounds will allow an examination of the redox properties as a function of solvent, metal and ligand. The metal and ligand effects are in general agreement with results in the literature.[17] No previous electrochemical data are available for these species, but comprehensive electrochemical studies have been performed on similar binuclear d^8 transition-metal complexes,[11–13] such as

† *Non-SI unit employed:* eV ≈ 1.60×10^{-19} J.

$[\{Ir(pz)(cod)\}_2]$ where pz is a bridging pyrazolyl ligand.[12] As will be discussed, the electrochemical behaviour for $[\{Ir(pz)(cod)\}_2]$, in which direct metal–metal intramolecular interactions are possible, is significantly different than that found for $[NBu_4][Ir_2(dcbmi)(cod)_2]$. The spectroelectrochemical data are in complete agreement with the chemical oxidation studies and in addition establish the site of electron transfer for these complexes.

Experimental

Equipment and Techniques.—Electrochemical experiments were performed with either a BAS-100A or an EG&G Princeton Applied Research 273 potentiostat/galvanostat coupled to an EG&G Princeton Applied Research model RE0091-XY recorder and an IBM PS/2 model 50 computer. A platinum-button working electrode, approximate area 0.008 cm^2, a platinum-wire counter electrode and a saturated calomel reference electrode (SCE) separated from the solution with a bridge comprised the three-electrode system. All potentials are reported *vs.* the SCE and have a precision of 0.010 V. Ferrocene was also used as an internal standard. The concentration of supporting electrolyte was 0.2 mol dm^{-3} unless otherwise stated. Bulk electrolysis experiments were carried out in a two-compartment cell with a large platinum working electrode, platinum counter electrode and a SCE reference electrode separated from the solution by a bridge.

Electronic spectroelectrochemical data were recorded with a Perkin-Elmer Lambda 3B UV/VIS spectrometer, interfaced to an IBM PS/2 model 60 computer with PECSS software, using a BAS CV-27 potentiostat coupled to an IBM 7427 MT X-Y-T recorder. Infrared spectroelectrochemical data were recorded with a Nicolet 510 FT-IR spectrometer using the same electrochemical apparatus. The electrodes in the spectroelectrochemical cell were a large platinum minigrid working electrode, a platinum-wire counter electrode and a platinum-wire pseudo-reference electrode. The supporting electrolyte concentration was 0.2 mol dm^{-3} unless otherwise stated. The UV/VIS data are presented as relative absorbance since compensation for the presence of the electrode (with 50% transmittance) and the tail of the solvent absorbance band was not performed. The IR results are presented as difference spectra and consequently these effects are removed.

The electrochemical cells were all laboratory built and designed for analysis of air-sensitive species.[18,19] All solid and solution transfers were carried out by standard Schlenk methodologies.[20] Conventional UV/VIS and IR measurements were performed with cells designed for inert-atmosphere measurements. X-Ray photoelectron spectra were recorded on a Vacuum Generators ESCA III spectrometer using Kα radiation as a source of photons. The apparatus was equipped with a PDP computer system for data acquisition. Peaks in the resulting spectra were deconvoluted using the Doniach–Sunjic formula,[21] to account for relaxation effects. Conductivity measurements were performed on pressed pellets using the van der Pauw method.[22] A Keithley 175 electrometer was used to measure voltage and a Keithley 610c electrometer to measure current. Constant current was generated with a Sambrook Engineering source. Silver epoxy resin was used for contacts.

Rhodium and Iridium Complexes.—The complexes $[NBu_4][M_2(dcmbi)(CO)_4]$, $[NBu_4][M_2(dcbmi)(cod)_2]$ (M = Rh or Ir) and $[NBu_4][Rh_2(dcbmi)(CO)_2(PPh_3)_2]$ were synthesised and characterized by published methods.[2]

$[NBu_4]_{0.5}[Ir_2(dcbmi)(CO)_4]\cdot 0.5CH_3CN$. A solution of $[NBu_4][Ir_2(dcbmi)(CO)_4]$ (200 mg) in CH_3CN (10 cm^3) was placed at the working electrode and a 0.1 mol dm^{-3} solution (10 cm^3) of NBu_4PF_6 in CH_3CN was used at the counter electrode of an electrochemical cell designed for bulk electrolysis under an inert atmosphere. A constant current of 15 μA was applied for 1 week and during this period a black solid formed on the working electrode. The solid was removed from the electrode, rinsed with acetonitrile in a Schlenk filter, and vacuum dried [Found (Calc. for $C_{19}H_{22.5}Ir_2N_3O_8$): C, 27.9 (28.3); H, 2.75 (2.80); Ir, 47.7 (47.7); N, 5.30 (5.20%)]. The yield was between 25 and 50%.

$[NPr_4]_{0.5}[Ir_2(dcbmi)(CO)_4]\cdot 0.25CH_3CN$. A similar procedure was used [Found (Calc. for $C_{16.5}H_{17.75}Ir_2N_{2.75}O_8$): C, 25.5 (25.8); H, 2.35 (2.35); N, 4.95 (5.00%)]. The yield was between 25 and 50%.

$[Rh_2(dcbmi)(CO)_4]\cdot H_2O$. The electrochemical procedure described above produces a dark red solid when $[NBu_4][Rh_2(dcbmi)(CO)_4]$ is used as the starting material. Alternatively this mixed-valence compound can be prepared by treating equimolar quantities of $[NBu_4][Rh_2(dcbmi)(CO)_4]$ with a suitable chemical oxidizing agent, such as $[p\text{-}CH_3C_6H_4N_2][BF_4]$, $[C_7H_7][BF_4]$ or $[NO][BF_4]$ in acetonitrile. A typical reaction is described. A solution of $[C_7H_7][BF_4]$ (0.1 mmol) in CH_3CN (10 cm^3) was slowly added to a solution of $[NBu_4][Rh_2(dcbmi)(CO)_4]$ (0.1 mmol) in CH_3CN (10 cm^3) under an inert atmosphere. The reaction mixture was stirred for 0.5 h and the dark red precipitate that formed was filtered off, rinsed with acetonitrile and vacuum dried. Yield 50% [Found (Calc. for $C_{10}H_5N_2O_9Rh_2$): C, 23.5 (23.9); H, 1.25 (1.00); N, 4.95 (5.55%)]. IR (KBr pellet): ν(CO) 2090s, 2026s; ν_{asym}(CO) 1664 cm^{-1}.

$[ttf][Rh_2(dcbmi)(CO)_4]$. A solution of $[ttf]_3[BF_4]_2$ (94 mg, 0.12 mmol) in acetonitrile (35 cm^3) was added dropwise to a solution of $[NBu_4][Rh_2(dcbmi)(CO)_4]$ (182 mg, 0.25 mmol) in acetonitrile (10 cm^3). A dark dichroic (blue-red) solid precipitated immediately, but the solution was stirred for 0.5 h. After this time the solid was filtered off, rinsed with acetonitrile and vacuum dried. Yield 120 mg (70%) [Found (Calc. for $C_{16}H_7N_2O_8Rh_2S_4$): C, 27.6 (27.9); H, 1.20 (1.00); N, 4.20 (4.05%)]. IR (KBr pellet): ν(CO) 2080s, 2053s, 2015s, 1983s; ν_{asym}(CO) 1674 cm^{-1}.

Materials.—The acetonitrile, dichloromethane and tetrahydrofuran (thf) used for electroanalysis were purchased (Aldrich) as spectroscopic grade, purified and dried by standard methods[23,24] stored over calcium hydride (CH_3CN), phosphorus pentaoxide (CH_2Cl_2), or sodium–benzophenone (thf) under an inert atmosphere and distilled just prior to use. Tetrabutylammonium perchlorate was purchased from Fluka, doubly recrystallized from ethanol and dried in a vacuum oven at 50 °C.

Results

$[NBu_4][M_2(dcbmi)(cod)_2]$ (M = Rh *or* Ir).—Fig. 1(*a*) shows the square-wave voltammogram obtained for $[NBu_4][Ir_2(dcbmi)(cod)_2]$ in thf and NBu_4ClO_4. Only one oxidation process (wave 1) is found up to the solvent limit, at E_{pa} = 0.93 V *vs.* SCE, with $E_{pa} - E_{pa/2}$ = 96 mV. Similar results are obtained by cyclic voltammetry, with only one wave being found at E_{pa} = 0.81 V. This wave has an $E_{pa} - E_{pa/2}$ = 91 mV. There are no coupled reduction waves associated with the oxidation of $[Ir_2(dcbmi)(cod)_2]^-$ in the cyclic voltammogram, and upon multiple scans passivation of the electrode surface after scanning positive of wave 1 is indicated. However, the electrode could be cleaned after each run by application of a negative (−1.5 V) potential. No reduction processes are observed for $[NBu_4][Ir_2(dcbmi)(cod)_2]$ up to −2.5 V *vs.* SCE in thf.

Bulk electrolysis studies were performed and oxidation at potentials positive of wave 1 gave a total of 1.7 ± 0.4 electrons per $[Ir_2(dcbmi)(cod)_2]^-$. The large error reflects the use of a dilute solution in the bulk electrolysis experiment to minimize the surface effects. Given that n = 2, the most significant feature of wave 1 is the value of $E_{pa} - E_{pa/2}$ in either the square-wave or the cyclic voltammetric experiments. The values are much larger than the 45 or 29 mV expected for a simple two-electron transfer

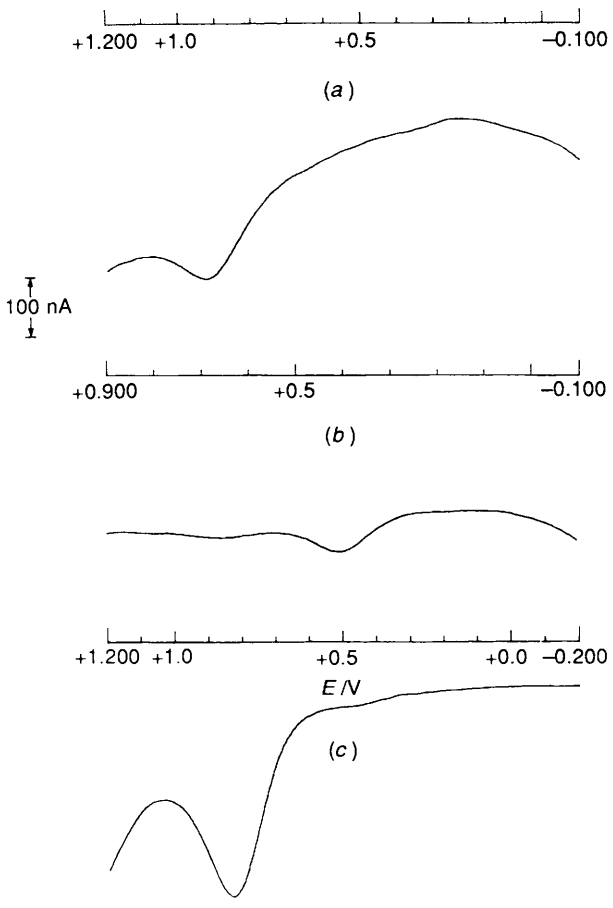

Fig. 1 Square-wave voltammograms of (*a*) a 9.57 × 10^{-4} mol dm^{-3} solution of $[NBu_4][Ir_2(dcbmi)(cod)_2]$ in 0.28 mol dm^{-3} NBu_4ClO_4, thf, (*b*) a 3.55 × 10^{-4} mol dm^{-3} solution of $[NBu_4][Rh_2(dcbmi)(cod)_2]$ in 0.24 mol dm^{-3} NBu_4ClO_4, CH_3CN and (*c*) a 9.81 × 10^{-4} mol dm^{-3} solution of $[NBu_4][Rh_2(dcbmi)(CO)_2(PPh_3)_2]$ in 0.28 mol dm^{-3} NBu_4ClO_4, CH_2Cl_2. For all measurements, the a.c. amplitude is 25 mV, the frequency 15 Hz and the step 4 mV

in square-wave[25] or cyclic measurements,[26,27] and are not due to solution resistance.* The large value of $E_{pa} - E_{pa/2}$ can be explained by either slow electron-transfer kinetics, chemical reaction(s) coupled to the two-electron transfer process, surface passivation, or any combination of these effects. Efforts were not made to distinguish between these processes.

The electrochemical properties of $[Ir_2(dcbmi)(cod)_2]^-$ in CH_2Cl_2 and CH_3CN, NBu_4ClO_4 are similar to those observed in thf, NBu_4ClO_4. Only wave 1 is found and by square-wave voltammetry the value of E_{pa} is 0.88 V *vs.* SCE in CH_2Cl_2. A large negative shift in potential is found when CH_3CN is the solvent and under these conditions E_{pa} is 0.16 V. The values of $E_{pa} - E_{pa/2}$ are 84 and 111 mV in CH_2Cl_2 and CH_3CN, respectively.

The electrochemical response for $[Rh_2(dcbmi)(cod)_2]^-$ matches that of the iridium analogue, as shown in Fig. 1(*b*) which is the square-wave voltammogram obtained in CH_3CN, NBu_4ClO_4. In this case, wave 1 is observed at $E_{pa} = 0.40$ V with $E_{pa} - E_{pa/2} = 67$ mV. Only one broad oxidation wave (wave 1) is found by cyclic voltammetry for this complex and E_{pa} for wave 1 is 0.44 and 0.80 V in CH_3CN and CH_2Cl_2, respectively. Note that, in CH_3CN, wave 1 is again shifted to more negative potentials. Bulk electrolysis of $[Rh_2(dcbmi)(cod)_2]^-$ under dilute conditions to minimize passivation of the electrode gives values of n of 1.9 ± 0.4 electrons per compound in CH_3CN. The electrochemical data are summarized in Table 1.

For both compounds the negative shift in E_{pa} when CH_3CN is the solvent can be explained by addition of CH_3CN to the oxidation product.[28] This was verified by titrating $[M_2(dcbmi)(cod)_2]^-$ (M = Rh or Ir) in thf or CH_2Cl_2 with CH_3CN, NBu_4ClO_4 and monitoring E_{pa} by cyclic voltammetry. It was observed that E_{pa} shifted by 68 and 85 mV per ten-fold change in the concentration of CH_3CN, for M = Ir or Rh respectively. Since $n = 2$, these data imply that 2.1 ± 0.5 and 2.8 ± 0.7 CH_3CN ligands are added for M = Ir and Rh, respectively, in the oxidation process. The different results may reflect the inherent differences between rhodium and iridium, but the surface effects for the rhodium species are also larger and result in a higher degree of uncertainty. Consequently the significance of the difference is not clear.

The spectroelectrochemical data† for oxidation of $[Ir_2(dcbmi)(cod)_2]^-$ in CH_3CN, NBu_4ClO_4 from 200 to 850 nm were monitored. The salt $Na_2Hdcbmi$ in water has a band at 262 nm, while $[Ir_2(dcbmi)(cod)_2]^-$ has absorption bands at 275 and 240 nm in CH_3CN in the UV region. Both of the UV bands of $[Ir_2(dcbmi)(cod)_2]^-$ decrease and shift slightly upon oxidation and the spectrum of the oxidized species is characterized by bands at 271 and 237 nm. If the potential is set to −1.20 V, after oxidation, the original spectrum is regenerated. Hence, on this time-scale $[Ir_2(dcbmi)(cod)_2]^-$ is generated from the oxidized species and any chemical reactions associated with electron transfer are reversible. Consequently, loss of either cod or $dcbmi^{3-}$ upon oxidation is unlikely. Since passivation of the electrode occurs upon oxidation of $[Ir_2(dcbmi)(cod)_2]^-$, abstraction of a full two electrons was not possible. The data presented correspond to the abstraction of two electrons from approximately half of the complex in the thin-layer region. Although not observed in the voltammetric experiments, the charge passed in the spectroelectrochemical experiments could also be interpreted as complete formation of the neutral, one-electron oxidation product. Unfortunately, the spectral changes are such that distinction between complete formation of $[Ir_2(dcbmi)(cod)_2]$ and partial formation of $[Ir_2(dcbmi)(cod)_2]^+$ is not possible.

Although $[Ir_2(dcbmi)(cod)_2]^-$ does have an absorption band in the visible region no spectral changes were observed from 850 to 325 nm upon oxidation. This is due to the small absorption coefficient[2] of the visible band. Spectroelectrochemical data for the oxidation of $[Rh_2(dcbmi)(cod)_2]^-$ are similar to those for $[Ir_2(dcbmi)(cod)_2]^-$ and are summarized in Table 2.

The spectral changes observed for the oxidation of $[M_2(dcbmi)(cod)_2]^-$ suggest that the oxidation is metal and not ligand centred. This is based on the relatively small spectral changes found in the UV region and that no evidence for formation of a radical was found in the visible region. Formation of radical species for metalloporphyrins[29–31] and other nitrogen heterocyclic systems[31] typically results in the formation of strong absorption bands in the 600–850 nm region. On the other hand, the small spectral changes in the UV region are indicative of a change of electron density on the metal atoms.

The electrochemical and spectroelectrochemical data for $[NBu_4][M_2(dcbmi)(cod)_2]$ are consistent with the electron-transfer mechanism presented in Scheme 1. The oxidation is a two-electron process that results in generation of the dinuclear metal(II) species, $[M_2(dcbmi)(cod)_2]^+$. Following formation of $[M_2(dcbmi)(cod)_2]^+$, depending upon the solvent, co-

* Ferrocene was added to the solution as an internal standard. A reversible wave was observed with $E_p - E_{p12} = 78$ and 60 mV for the anodic and cathodic wave, respectively.

† In all spectroelectrochemical experiments the potential is stepped to a pre-determined point while monitoring the current–time response. Consequently the total charge is monitored to determine the number of electrons transferred.

Table 1 Electrochemical data[a]

Complex	Solvent	Wave[b] 1	2	3	4	5	6	*c*
$[NBu_4][Rh_2(dcbmi)(cod)_2]$	CH_3CN	0.44 (0.40)						0.38
	CH_2Cl_2	0.80 (0.81)						0.46
$[NBu_4][Rh_2(dcbmi)(CO)_4]$	CH_3CN	0.64	0.70	0.75	0.90	−0.34[d]		0.38
	CH_2Cl_2	0.94						0.36
	thf	0.96						0.41
$[NBu_4][Rh_2(dcbmi)(CO)_2(PPh_3)_2]$	CH_3CN	0.63 (0.57)						0.41
	CH_2Cl_2	0.88 (0.83)						0.45
$[NBu_4][Ir_2(dcbmi)(cod)_2]$	CH_3CN	0.16[e]						0.40
	CH_2Cl_2	0.88[e]						0.52
	thf	0.93[e]						0.34
$[NBu_4][Ir_2(dcbmi)(CO)_4]$	CH_3CN	0.03	0.46	0.75		0.07	−0.30	0.39
	CH_2Cl_2	0.36	0.78	0.98		0.55	0.04	0.49
	thf	0.54		1.12		0.46	0.25	0.72[f]

[a] Potentials relative to SCE as measured by cyclic voltammetry. Square-wave measurements are in parentheses. [b] Value of E_p at 100 mV s^{-1}. [c] Value of $E_{\frac{1}{2}}$ for ferrocene. [d] Only observed upon multiple scans. See text. [e] E_p by square-wave voltammetry. [f] Referenced *vs.* platinum-wire pseudo-reference.

Table 2 Spectroelectrochemical data[a]

Complex	*n*	Potential[b]/ V	λ_{max}[c]/ nm	$\tilde{\nu}$/cm^{-1}
$[NBu_4][Rh_2(dcbmi)(cod)_2]$		None	273	
	1	1.60	273	
$[NBu_4][Rh_2(dcbmi)(CO)_4]$		None	277	2000, 2071
	1	1.30	240, 276	2017, 2089
$[NBu_4][Rh_2(dcbmi)(CO)_2(PPh_3)_2]$[d]		None	240	
	1	1.60	280	
$[NBu_4][Ir_2(dcbmi)(cod)_2]$		None	240, 275	
	1	1.20	237, 271	
$[NBu_4][Ir_2(dcbmi)(CO)_4]$		None	241, 274	1989, 2064
	1	0.70	241, 274[e]	2010, 2027, 2090

[a] Spectra measured in CH_3CN, 0.2 mol dm^{-3} NBu_4ClO_4. [b] Potential at the working electrode relative to a platinum-wire pseudo-reference electrode. [c] Spectra are tabulated for the UV region only. See text. [d] Small spectral changes observed. See text. [e] Bands all decrease in intensity upon oxidation, but do not shift.

ordination may occur as indicated. It is interesting to note that stabilization of rhodium(II) and iridium(II) species by CH_3CN following electrochemical generation has been previously reported.[12,18,32,33]

The electrochemical data for $[Ir_2(dcbmi)(cod)_2]^-$ are significantly different from those observed for $[\{Ir(pz)(cod)\}_2]$.[12]

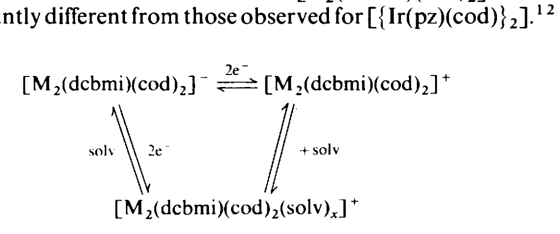

Scheme 1 M = Rh or Ir, solv = solvent

The complex $[\{Ir(pz)(cod)\}_2]$ has a reversible, single electron transfer at $E_{\frac{1}{2}}$ = 0.42 V and a chemically irreversible process at E_{pa} = 1.28 V *vs.* Ag–AgCl in CH_2Cl_2 on the cyclic voltammetric time-scale. Bulk electrolysis positive of the *first* oxidation wave results in the generation of a dinuclear iridium(II) complex which reacted with CH_2Cl_2. A strong dependence of the electrochemical response upon the solvent was also observed for $[\{Ir(pz)(cod)\}_2]$ and in CH_3CN a reversible two-electron transfer process at $E_{\frac{1}{2}}$ = 0.262 V *vs.* Ag–AgCl was found. The solvent dependence was attributed to the addition of CH_3CN to the electrogenerated iridium(II) species.

The reason for the different electrochemical behaviour between $[Ir_2(dcbmi)(cod)_2]^-$ and $[\{Ir(pz)(cod)\}_2]$ is due to the direct metal–metal interaction in the latter. The highest occupied molecular orbital (HOMO) for $[\{Ir(pz)(cod)\}_2]$ is a metal–metal antibonding orbital, and hence oxidation favours metal–metal bond formation. Consequently, electrogeneration of a reactive metal–metal bonded species is observed which can undergo significantly different chemical reactions. For $[Ir_2(dcbmi)(cod)_2]^-$, direct metal–metal bonding within the molecule is not possible and hence oxidation results in a distinct species. The lack of significant surface effects for $[\{Ir(pz)(cod)\}_2]$ also suggests different solubility of the electrogenerated species.

$[NBu_4][Rh_2(dcbmi)(CO)_2(PPh_3)_2]$.—The cyclic voltammogram obtained for $[NBu_4][Rh_2(dcbmi)(CO)_2(PPh)_3)_2]$ in CH_3CN, NBu_4ClO_4 at a scan rate of 100 mV s^{-1} has one very broad oxidation wave centred at 0.63 V *vs.* SCE (wave 1) and no associated re-reduction processes. In addition, no reduction waves are found upon scanning in a negative direction.

The value of $E_{pa} - E_{pa/2}$ for wave 1 is very large and difficult to measure accurately, which again may be due to one of several different processes. A similar solvent dependence is found for this compound and, for example, E_{pa} = 0.88 V *vs.* SCE in CH_2Cl_2, NBu_4ClO_4. Square-wave voltammetry is consistent with the cyclic voltammetric results, and for example a wave at E_{pa} = 0.83 V *vs.* SCE is found with $E_{pa} - E_{pa/2}$ = 106 mV in CH_2Cl_2. This is shown in Fig. 1(*c*). Multiple cyclic voltammetric scans again show a rapid decrease in the current, attributed to passivation of the electrode following oxidation. Bulk electrolysis studies under dilute conditions give a value of *n* of 1.0 ± 0.4 electrons per complex. These data are summarized in Table 1.

Only small currents are obtained when spectroelectrochemical experiments are performed on $[NBu_4][Rh_2(dcbmi)(CO)_2(PPh_3)_2]$ due to passivation of the electrode surface upon oxidation and corresponding small spectral changes are found. However the changes that are observed are significant. The original complex has an absorption band at 240 nm which decreases upon oxidation, while a new band is formed at 280 nm, with an isosbestic point at 245 nm. Re-reduction results in generation of the original spectrum, implying regeneration of

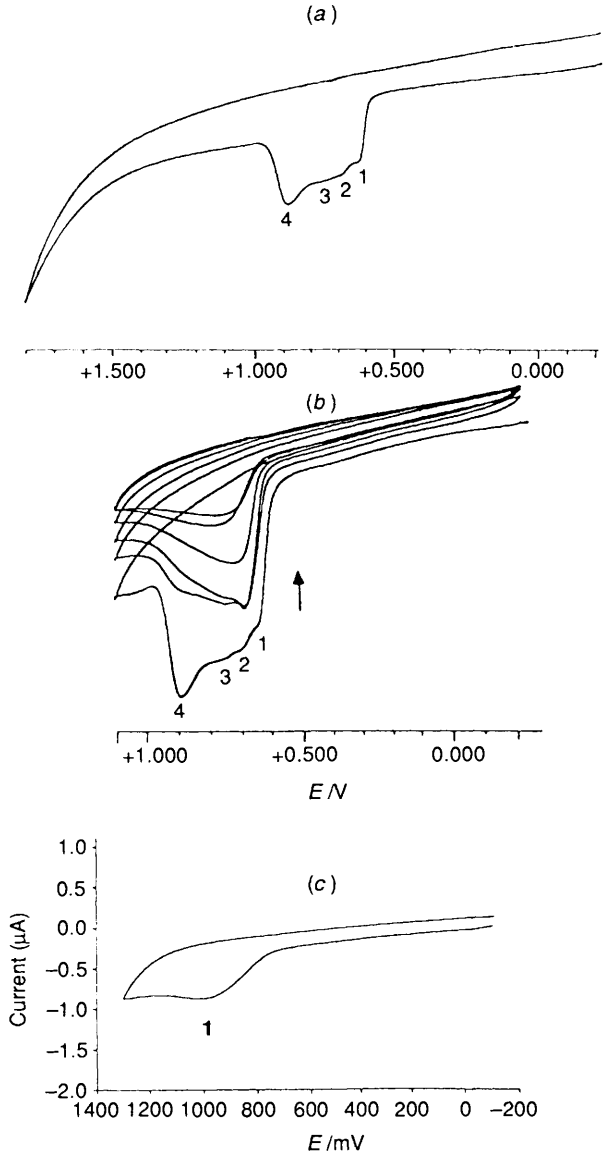

Fig. 2 (*a*) Cyclic voltammogram of a 8.80 × 10^{-4} mol dm^{-3} solution of $[NBu_4][Rh_2(dcbmi)(CO)_4]$ in 0.21 mol dm^{-3} NBu_4ClO_4, CH_3CN. Scan rate 100 mV s^{-1}. (*b*) Multiple cyclic voltammetric scans obtained for the same solution (*a*). (*c*) Cyclic voltammogram of a 7.80 × 10^{-4} mol dm^{-3} solution of $[NBu_4][Rh_2(dcbmi)(CO)_4]$ in 0.20 mol dm^{-3} NBu_4ClO_4, CH_2Cl_2. Scan rate 100 mV s^{-1}

the starting anion and consequently no significant degradation of the complex upon oxidation.

The cyclic voltammetric and spectroelectrochemical data suggest that a mechanism similar to that presented in Scheme 1, but with a value of *n* of one, is valid for $[NBu_4][Rh_2(dcbmi)(CO)_2(PPh_3)_2]$. Hence, following oxidation, addition of solvent can occur and titration experiments with CH_3CN indicate the addition of 1.9 ± 0.5 molecules of solvent after oxidation.

$[NBu_4][Rh_2(dcbmi)(CO)_4]$.—Fig. 2(*a*) shows the cyclic voltammetric response from −0.20 to 1.8 V for $[NBu_4][Rh_2(dcbmi)(CO)_4]$ in CH_3CN, NBu_4ClO_4 at a scan rate of 100 mV s^{-1}. The oxidation of this complex is complicated and consists of four combined oxidation waves at E_{pa} = 0.64, 0.70, 0.75 and 0.90 V *vs.* SCE [waves 1–4, Fig. 2(*a*)] on the first scan. No re-reduction waves are found after scanning positive of waves 1–4. In addition, no reduction processes are found for this complex up to −2.0 V *vs.* SCE.

The cyclic voltammogram for $[NBu_4][Rh_2(dcbmi)(CO)_4]$ shows significant changes on the second and subsequent sweeps if multiple scans are performed, as shown in Fig. 2(*b*). On the second sweep the oxidation has two combined waves at E_{pa} = 0.68 and 0.88 V *vs.* SCE. The current on the second sweep is greatly diminished relative to the first. In subsequent scans one broad wave is observed and the current for this wave continues to decrease. At the same time a small re-reduction wave grows in at −0.34 V *vs.* SCE [wave 5, not shown in Fig. 2(*b*)]. After approximately six scans the cyclic voltammograms become identical. The electrode can be cleaned by scanning to potentials negative of −1.00 V and under these conditions multiple scans are identical to the initial scan.

Electrochemical characterization of waves 1–4 cannot be accurately performed due to the combined nature of these processes. However, the electrochemical data do demonstrate that waves 2 and 3 are due to intermediate species. For example, the peak currents for waves 1 and 4 are significantly greater than those for waves 2 and 3 and at scan rates below 60 mV s^{-1} only waves 1 and 4 are observed. Further evidence for assigning waves 2 and 3 to intermediate species is that bulk electrolysis of $[NBu_4][Rh_2(dcbmi)(CO)_4]$ in CH_3CN at a potential positive of wave 4 gives a value of *n* of 2.2 ± 0.4 electrons per molecule. The bulk electrolysis experiments were carried out in dilute conditions which accounts for the large experimental error.

The oxidative cyclic voltammetric behaviours of $[Rh_2(dcbmi)(CO)_4]^-$ in CH_2Cl_2 or thf are similar, but distinct from that when CH_3CN is the solvent. This is shown in Fig. 2(*c*), which is representative of the cyclic voltammetric data in CH_2Cl_2. Under these conditions only one broad oxidation wave is observed [wave 1, Fig. 2(*c*)] at 0.94 V *vs.* SCE. The value of $E_{pa} - E_{pa/2}$ for wave 1 is 98 mV. No re-reduction waves are found after scanning positive of wave 1 and multiple scans indicate passivation of the electrode surface after oxidation. These data are summarized in Table 1.

The strong dependence of the electrochemical behaviour on the solvent conditions is due to the addition of CH_3CN upon oxidation and the stabilization of one or more intermediate species by CH_3CN. Titration of solutions of $[NBu_4][Rh_2(dcbmi)(CO)_4]$ in CH_2Cl_2 with MeCN shows that the potential for wave 1 shifts by 99 mV per ten-fold increase in the concentration of CH_3CN. The classical interpretation of these data is that 3.3 ± 0.5 molecules of CH_3CN are added to the oxidation product,[12,28] assuming *n* is 2. The analysis is not straightforward, however, since addition of CH_3CN also causes wave 1 to split in four waves. When the solvent is approximately 30% CH_3CN (by volume) the cyclic voltammogram is the same as that obtained in pure CH_3CN, NBu_4ClO_4.

Fig. 3(*a*) shows the spectral changes that occur from 320 to 200 nm upon oxidation of $[NBu_4][Rh_2(dcbmi)(CO)_4]$ by one electron. This complex is characterized by an absorption band at 277 nm which decreases upon oxidation and slightly shifts. At the same time a new band appears at 240 nm and isosbestic points are observed at 250 and 232 nm. No significant spectral changes were observed in the visible region due to the low absorption coefficients of the bands. Fig. 3(*b*) shows the corresponding changes in the M–CO stretching region of the infrared spectrum upon oxidation of $[NBu_4][Rh_2(dcbmi)(CO)_4]$ in CH_2Cl_2. In this solvent the complex has two Rh–CO bands at 2071 and 1999 cm^{-1}, which upon oxidation decrease to the baseline,* while new bands are observed at 2089 and 2018 cm^{-1}. This shift to higher wavenumbers is fully consistent with metal-centred oxidation.

For both the UV/VIS and IR spectroelectrochemical experiments, reduction of the oxidized species at −0.50 V results in

* The decrease in the original bands is represented as a % transmission greater than 100% while the increase in the new bands is represented as a % transmission less than 100% in the difference spectra.

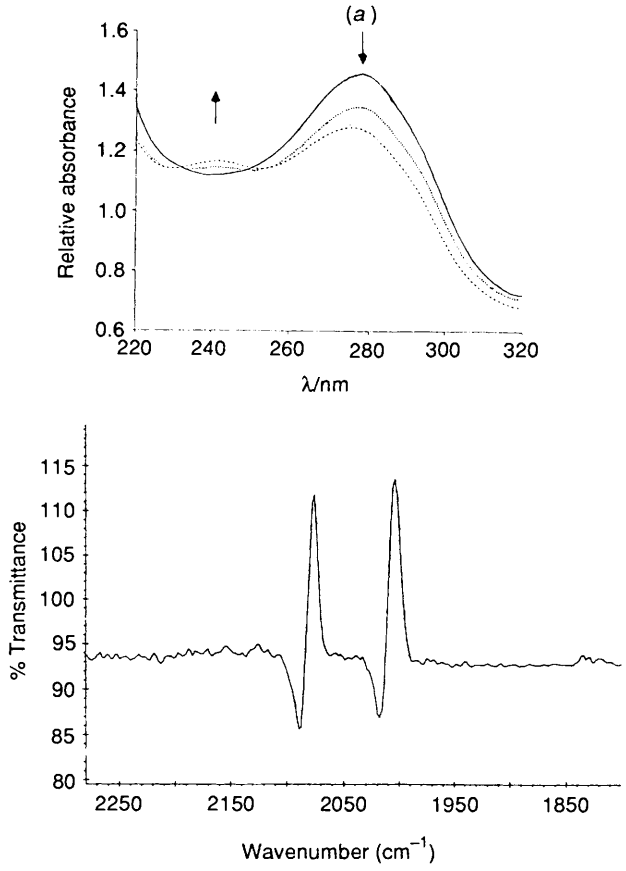

Fig. 3 (*a*) Spectral changes observed from 320 to 220 nm upon oxidation of $[NBu_4][Rh_2(dcbmi)(CO)_4]$ at 1.30 V *vs.* a platinum wire in CH_3CN, NBu_4ClO_4. (——) No applied potential, (· · · ·) t = 50 s, (– – –) t = 100 s. (*b*) Infrared spectral changes for $[NBu_4][Rh_2(dcbmi)(CO)_4]$ upon oxidation at 1.50 V *vs.* Pt wire in CH_2Cl_2

regeneration of $[Rh_2(dcbmi)(CO)_4]^-$. This reversibility demonstrates that any chemical reactions associated with electron transfer are reversible, which suggests that neither CO nor $dcbmi^{3-}$ is lost upon oxidation. The IR spectroelectrochemical data also demonstrate that the basic geometry of the complex is not altered upon oxidation in non-co-ordinating solvents such as CH_2Cl_2.

Chemical oxidation or preparative bulk electrolysis of $[Rh_2(dcbmi)(CO)_4]^-$, where the concentration of the starting material is significantly larger, results in the generation of an insoluble precipitate. The IR data and the elemental analysis best fit the formulation of this insoluble product as $[Rh_2(dcbmi)(CO)_4]$, as indicated in reaction (1). The M–CO

$$[Rh_2(dcbmi)(CO)_4]^- \overset{e^-}{\rightleftharpoons} [Rh_2(dcbmi)(CO)_4] \quad (1)$$

stretching region in the infrared spectra of this product has two bands at 2090 and 2026 cm^{-1}, in agreement with oxidation at the metal centre. These data are also in agreement with the solution infrared spectroelectrochemical data. Interestingly, bulk magnetic susceptibility measurements indicated that the compound is diamagnetic. Since $[Rh_2(dcbmi)(CO)_4]$ has an odd number of electrons, the magnetic susceptibility data imply an intermolecular metal–metal bond between rhodium(II) centres in the solid state. In agreement, formation of an Ir^{II}–Ir^{II} intermolecular metal bond upon electrochemical oxidation of flat, anionic iridium(I) complexes has been reported.[32]

The chemical, electrochemical and spectroelectrochemical data for $[NBu_4][Rh_2(dcbmi)(CO)_4]$ are consistent with the mechanism presented in Scheme 2. Following initial oxidation (wave 1), $[Rh_2L(CO)_4]$ is formed which will add solvent (CH_3CN) and/or precipitate. The precipitation of this species accounts for the passivation of the electrode surface and wave 5 is assigned to the reduction of this species. Waves 2–4 cannot be exactly assigned, but correspond to the abstraction of a second electron from the electrogenerated neutral species. Hence, a competition between solvation of the rhodium(II) ions and formation of an insoluble metal–metal bonded species occurs upon oxidation.

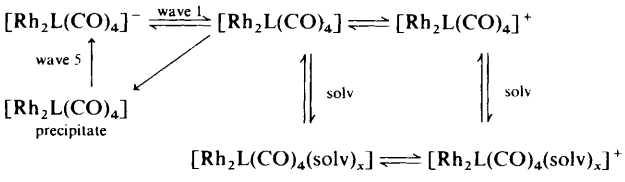

Scheme 2 L = $dcbmi^{3-}$, solv = solvent

When $[Rh_2(dcbmi)(CO)_4]^-$ was treated with $[ttf]_3[BF_4]$ the insoluble salt $[ttf][Rh_2(dcbmi)(CO)_4]$ formed immediately. The pressed-pellet conductivity at room temperature was 6×10^{-5} ohm^{-1} cm^{-1}. The stacking of the ttf^+ radical cations is probably responsible for the conductivity in this solid.[15,16]

$[NBu_4][Ir_2(dcbmi)(CO)_4]$.—Fig. 4(*a*) shows the cyclic voltammogram obtained for $[NBu_4][Ir_2(dcbmi)(CO)_4]$ in CH_3CN, NBu_4ClO_4 upon scanning from −0.20 to 1.20 to −1.00 V *vs.* SCE at 100 mV s^{-1}. There are three oxidation waves observed at E_{pa} = 0.03, 0.46 and 0.75 V *vs.* SCE [waves 1–3, Fig. 4(*a*)]. In addition, two re-reduction waves are found at E_{pc} = 0.07 and −0.30 *vs.* SCE [waves 5 and 6, Fig. 4(*a*)] after scanning positive of wave 3. The currents for waves 5 and 6 are less than those of waves 1 and 3. No reduction waves are found for $[NBu_4][Ir_2(dcbmi)(CO)_4]$ upon scanning in a negative direction.

Wave 1 is characterized as a diffusion-controlled, one-electron transfer evidenced by a constant value of $i_p/v^{\frac{1}{2}}$ and a value of $E_{pa} - E_{pa/2}$ of 86 mV. After scanning positive of wave 1, wave 6 is observed and hence these processes are coupled. The value of ΔE_p for waves 1 and 6 is 303 mV, which is too large to consider the electron transfer as reversible.[26] The data are consistent, however, with a chemical reaction following oxidation (wave 1) and with wave 6 due to the re-reduction of the chemical reaction product.

Wave 2 is a small process on the shoulder of wave 3, and hence is difficult to characterize. Wave 3 appears to be a diffusion-controlled, one-electron process since $E_{pa} - E_{pa/2}$ = 82 mV and $i_p/v^{\frac{1}{2}}$ is a constant. However, there is some uncertainty in these values due to wave 2. Wave 5 is only observed after scanning positive of wave 3 and hence these processes are also coupled. The large value of ΔE_p between waves 3 and 5 again suggests that a chemical reaction follows this oxidation process (wave 3).

Cyclic voltammetric data for $[NBu_4][Ir_2(dcbmi)(CO)_4]$ in thf or CH_2Cl_2, NBu_4ClO_4 are similar to results in CH_3CN, and are summarized in Table 1. Note that the oxidation potentials are again shifted in a negative direction in CH_3CN relative to thf or CH_2Cl_2. In addition, the current for wave 2 is much less for both of the latter solvent systems.

Fig. 4(*b*) shows the results of multiple scans in the cyclic voltammogram of $[NBu_4][Ir_2(dcbmi)(CO)_4]$ in CH_2Cl_2, NBu_4ClO_4 upon scanning from −300 to 600 mV at 100 mV s^{-1}. An *increase* in the current for both waves 1 and 6 is observed under these conditions. In addition, both waves 1 and 6 shift to negative potentials and a new oxidation process appears to grow in at 0.30 V *vs.* SCE. The increase in current and the shift in potential are both significant features and are indicative of the formation of a conducting film on the electrode surface.[34–36] A similar response is obtained when the potential is scanned positive of wave 3. In this case the currents for waves 1, 3, 5 and 6 all increase on each successive scan. Multiple scans also

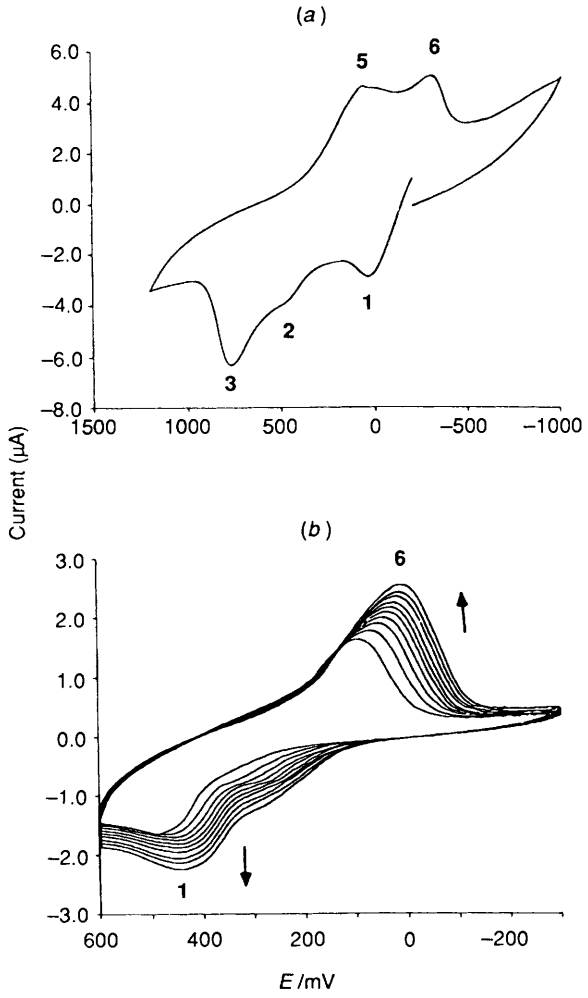

Fig. 4 (*a*) Cyclic voltammogram of a 1.77×10^{-4} mol dm^{-3} solution of $[NBu_4][Ir_2(dcbmi)(CO)_4]$ in 0.27 mol dm^{-3} NBu_4ClO_4, CH_3CN. Scan rate 100 mV s^{-1}. (*b*) Multiple cyclic voltammetric scans for a 4.04×10^{-4} mol dm^{-3} solution of $[NBu_4][Ir_2(dcbmi)(CO)_4]$ in 0.22 mol dm^{-3} NBu_4ClO_4, CH_2Cl_2. Scan rate 100 mV s^{-1}

indicate the formation of a conducting film on the electrode for both CH_3CN and thf solvent systems.

The spectroelectrochemical data for $[NBu_4][Ir_2(dcbmi)(CO)_4]$ are different from those of the rhodium analogue due to precipitation of the oxidized complex on the electrode surface. For example, in CH_2Cl_2, NBu_4ClO_4 upon the abstraction of one electron, the absorption bands at 274 and 241 nm for the original complex decrease in intensity to near background with no indication of the formation of new bands. In the spectral region 325–800 nm, $[Ir_2(dcbmi)(CO)_4]^-$ has absorption bands at 354 and 393 nm, and upon oxidation these bands also decrease. The salt $[NBu_4][Ir_2(dcbmi)(CO)_4]$ has M–CO bands in the infrared at 2063 and 1989 cm^{-1} in CH_2Cl_2 which also decrease to the baseline upon the abstraction of one electron. However, in this experiment two small bands at 2082 and 2025 cm^{-1} appear to form. Upon re-reduction at −0.05 V formation of the original complex is indicated in both the IR and UV/VIS studies. This implies that loss of either CO or dcbmi^{3-} does not occur following oxidation.

The electrochemical and spectroelectrochemical data for $[NBu_4][Ir_2(dcbmi)(CO)_4]$ are consistent with oxidation followed by solvation, similar to Scheme 2. The anion $[Ir_2(dcbmi)(CO)_4]^-$ can be oxidized up to two times (waves 1 and 2). The electrogenerated species react with solvent to form $[Ir_2(dcbmi)(CO)_4(solv)_x]$ or $[Ir_2(dcbmi)(CO)_4(solv)_x]^+$. Waves 3, 5 and 6 are assigned to oxidation or reduction of these species. Regeneration of $[Ir_2(dcbmi)(CO)_4]^-$ is ultimately

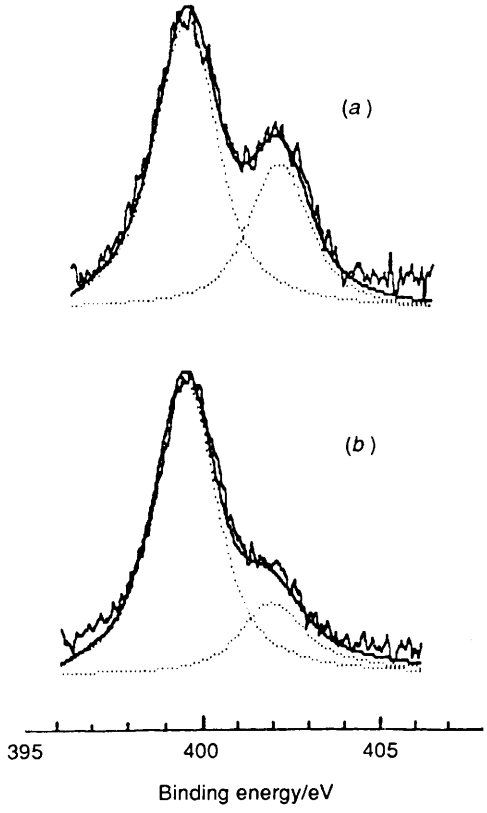

Fig. 5 X-Ray photoelectron spectra in the nitrogen region of (*a*) $[NBu_4][Ir_2(dcbmi)(CO)_4]$ and (*b*) $[NBu_4]_{0.5}[Ir_2(dcbmi)(CO)_4]$. Dotted lines represent deconvolution of spectra

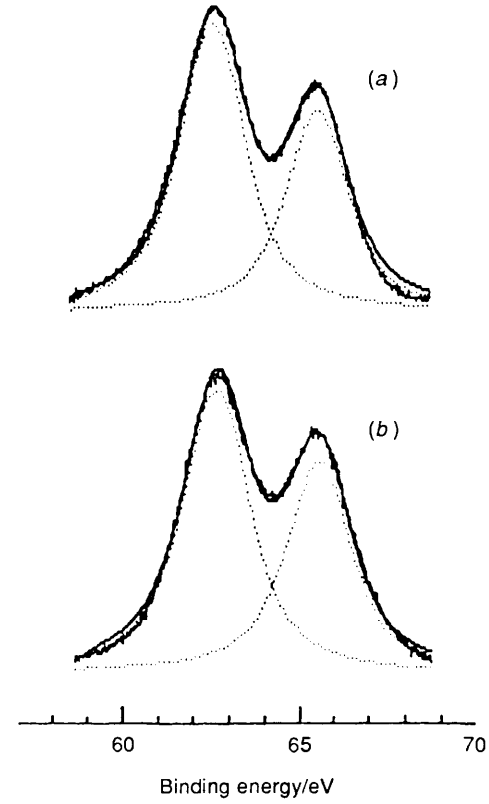

Fig. 6 X-Ray photoelectron spectra in the iridium region. Details as in Fig. 5

observed, hence the reduction steps (waves 5 and 6) result in a loss of solvent.

Table 3 XPS binding energies in the iridium and nitrogen region for $[NBu_4]_x[Ir_2(dcbmi)(CO)_4]$

Compound	Region	Binding energy/eV	Relative intensity
$[NBu_4][Ir_2(dcbmi)(CO)_4]$	Ir ($4f_{\frac{7}{2}}$)	62.50	1.00
	Ir ($4f_{\frac{5}{2}}$)	65.50	0.70
	N (1s) ring[a]	399.70	1.00
	N (1s) cation[b]	402.30	0.50
$[NBu_4]_{0.5}[Ir_2(dcbmi)(CO)_4]$	Ir ($4f_{\frac{7}{2}}$)	62.60	1.00
	Ir ($4f_{\frac{5}{2}}$)	65.55	0.75
	N (1s) ring[a]	399.65	1.00
	N (1s) cation[b]	401.95	0.24

[a] $dcbmi^{3-}$ bridging ligand. [b] Tetrabutylammonium cation.

In addition, a competing reaction exists between the oxidation product and the unoxidized complex to form the mixed-valence species $[\{Ir_2(dcbmi)(CO)_4\}_2]^-$, on the electrode surface as indicated by equation (2) where L is $dcbmi^{3-}$. This species

$$[Ir_2L(CO)_4] + [Ir_2L(CO)_4]^- \rightleftharpoons [\{Ir_2L(CO)_4\}_2]^- \quad (2)$$

can also be written as $[NBu_4]_{0.5}[Ir_2(dcbmi)(CO)_4]$ which was synthesised in large quantity to allow characterization.

Electrochemical oxidation of $[NBu_4][Ir_2(dcbmi)(CO)_4]$ in high concentrations as described in the Experimental section, results in formation of $[NBu_4]_{0.5}[Ir_2(dcbmi)(CO)_4]$. A similar result is obtained with $[NPr_4][Ir_2(dcbmi)(CO)_4]$. The stoichiometry of the partially oxidized iridium complexes was determined from elemental analysis and verified by the results of XPS studies, as shown in Figs. 5 and 6 and summarized in Table 3. Fig. 5(*a*) and 5(*b*) are the spectra of the 1s region of nitrogen for both the unoxidized and oxidized species, respectively. For the unoxidized species the peak in binding energy centred at 399.70 eV is due to the nitrogens in the heterocyclic ring (*i.e.* $dcbmi^{3-}$), while the peak at 402.30 eV is due to the nitrogen in the tetrabutylammonium cation. The intensity ratio of these two peaks is 1:0.5, in agreement with the formulation of the starting material as $[NBu_4][Ir_2(dcbmi)(CO)_4]$. The X-ray photoelectron spectrum of the oxidized species shows a slight shift in the peak due to the nitrogens in $dcbmi^{3-}$ to 399.65 eV, while the peak due to the nitrogen in NBu_4^+ shifts to 401.95 eV. In addition, the relative intensity of the two bands for this species is 1:0.24, in agreement with the formulation of the partially oxidized species as $[NBu_4]_{0.5}[Ir_2(dcbmi)(CO)_4]$. The use of XPS for quantitative analysis is well known,[37] but this represents a different approach for the determination of the degree of partial oxidation of non-stoichiometric materials.

Fig. 6 shows the results of XPS studies in the iridium region for both the oxidized and the unoxidized complex. In both cases the spectra can be fitted with a single type of iridium and only a slight decrease in binding energy is observed for $[NBu_4]_{0.5}[Ir_2(dcbmi)(CO)_4]$ relative to $[NBu_4][Ir_2(dcbmi)(CO)_4]$. It is not always the case that only a single type of iridium is observed in complexes of the form $[cation]_x[Ir_2L(CO)_4]$. With other bridging ligands two distinct types of iridium can be observed following partial oxidation.

The analysis of the XPS data implies that in solid $[NBu_4]_{0.5}[Ir_2(dcbmi)(CO)_4]$ both iridiums in the dinuclear unit are involved in the formation of stacks, resulting in a formal oxidation state of +1.25 per iridium atom. However, a definitive X-ray crystal structure has not yet been accomplished.

The infrared spectra of the oxidized solids are dominated by a band edge characteristic of semiconductive materials, which obscures most of the vibrational spectra. Isotropic conductivities measured on pressed pellets at room temperature were 8×10^{-5} ohm^{-1} cm^{-1} for $[NPr_4]_{0.5}[Ir_2(dcbmi)(CO)_4]$ and 2×10^{-5} ohm^{-1} cm^{-1} for $[NBu_4]_{0.5}[Ir_2(dcbmi)(CO)_4]$. For comparison purposes, the conductivities of the unoxidized samples, also measured as pressed pellets, are in the range of 10^{-7}–10^{-8} ohm^{-1} cm^{-1}, depending upon the cation. The conduction values obtained for $[cation]_{0.5}[Ir_2(dcbmi)(CO)_4]$ represent a lower limit, since for highly anisotropic systems the conductivity along the main axis can be two to three orders of magnitude higher than the averaged isotropic values.[15] A rapid decrease in the conductivity of the partially oxidized species was observed with time, probably due to the loss of solvent present in the structure. This effect is significant in the time required for the conductivity measurement and further implies that the values reported are a lower limit. The effect of the loss of solvent on the conductivity of partially oxidized tetracyanoplatinates[15] and other systems[38] has been previously reported.

It is interesting that the reaction of $[ttf]_3[BF_4]_2$ with $[NBu_4][Ir_2(dcbmi)(CO)_4]$ also produces $[NBu_4]_{0.5}[Ir_2(dcbmi)(CO)_4]$ in contrast to the rhodium analogue, which results in precipitation of the unoxidized $[ttf][Rh_2(dcbmi)(CO)_4]$. The lower oxidation potential of the iridium anion compared to that of the rhodium analogue accounts for this. Synthesis of the iridium material by chemical oxidation with $[ttf]_3[BF_4]_2$ results in a lower-purity product than that obtained by electrochemical methods.

Discussion

One dominating aspect of the electrochemical properties are the surface effects observed for these species. In all cases the spectroelectrochemical data indicated no significant degradation upon oxidation, which suggests the electrode effects are due to precipitation of either the electrogenerated neutral or cationic species. The iridium carbonyl derivative clearly shows formation of the conductive material $[NBu_4]_{0.5}[Ir_2(dcbmi)(CO)_4]$. As expected,[15] planarity of the complex and the large spatial size of iridium are necessary to form the mixed-valence delocalized stacked structures that result in the growth of a conducting material on the electrode surface. Therefore, of the complexes discussed in this present study, only $[Ir_2(dcbmi)(CO)_4]^-$ produces this type of material. The formation of this partially oxidized solid can be monitored by cyclic voltammetry and other electrochemical techniques and further characterization of the properties of this and related systems is in progress.

The results from this study also allow a comparison of the electron-transfer potential as a function of metal and ligand. When M is changed from Rh to Ir, the oxidation potential shifts to negative potentials by 240 mV for the cod derivative and by 610 mV for the carbonyl derivative. When the ligand system is changed from cod to either CO or PPh_3, the oxidation potential becomes more positive. This is consistent with a decrease in electron density on the metal due to co-ordination to the stronger π-acid ligands. In addition, a small negative shift (0.01 V in CH_3CN and 0.06 V in CH_2Cl_2) was also found upon replacing CO with PPh_3. These electrochemical trends are expected and consistent with data[17] relating redox potential to ligand and metal properties.

Acknowledgements

Acknowledgement is made by J. E. A. to the Donors of the Petroleum Research Fund, administered by the American Chemical Society, for the support of this research, and to Johnson Matthey for the loan of rhodium and iridium metal. J. C. B. acknowledges support from Comisión Asesora para la Investigacion Científica y Técnica (CAICYT) (PB85-008) and Dirrección General para la Investigación Científico y Técnica (DGICYT) (PB88-0252).

References

1 J. C. Bayón and G. Net, *NATO ASI Ser., Ser. B*, 1987, **168**, 365.

2 J. C. Bayón, G. Net, P. G. Rasmussen and J. B. Kolowich, *J. Chem. Soc., Dalton Trans.*, 1987, 3003.
3 G. Net, J. C. Bayón, W. M. Butler and P. G. Rasmussen, *J. Chem. Soc., Chem. Commun.*, 1989, 1022.
4 P. G. Rasmussen, J. B. Kolowich and J. C. Bayón, *J. Am. Chem. Soc.*, 1988, **110**, 7042.
5 L. S. Fox, J. L. Marshall, H. B. Gray and J. R. Winkler, *J. Am. Chem. Soc.*, 1987, **109**, 6901.
6 J. R. Winkler, J. L. Marshal, T. L. Netzel and H. B. Gray, *J. Am. Chem. Soc.*, 1986, **108**, 2263.
7 V. M. Miskowski, T. P. Smith, T. M. Loehxr and H. B. Gray, *J. Am. Chem. Soc.*, 1985, **107**, 7925.
8 D. L. Lichtenberger, A. S. Copenhaver, H. B. Gray, J. L. Marshall and M. D. Hopkins, *Inorg. Chem.*, 1988, **27**, 4488.
9 T. Brauns, C. Carriedo, J. S. Cockayne, N. G. Connelly, G. G. Herbora and A. G. Orpen, *J. Chem. Soc., Dalton Trans.*, 1989, 2049.
10 S. R. Stobart and R. D. Brost, *Inorg. Chem.*, 1989, **28**, 4307.
11 R. Seeber, G. Minghetti, M. J. Pilo, G. Banditelli and S. Zamponi, *J. Organomet. Chem.*, 1991, **402**, 413.
12 D. C. Boyd, G. S. Rodman and K. R. Mann, *J. Am. Chem. Soc.*, 1986, **108**, 1779.
13 A. Sykes and K. R. Mann, *J. Am. Chem. Soc.*, 1988, **110**, 8252.
14 W. A. Fordyce, K. H. Pool and G. A. Crosby, *Inorg. Chem.*, 1982, **21**, 1027.
15 *Extended Linear Chain Compounds*, ed. J. S. Miller, Plenum, New York, 1981, vol. 1.
16 A. O. Patil, A. J. Heeger and F. Wudl, *Chem. Rev.*, 1988, **88**, 183.
17 A. B. P. Lever, *Inorg. Chem.*, 1990, **29**, 1271.
18 J. E. Anderson and T. P. Gregory, *Inorg. Chem.*, 1989, **28**, 3905.
19 J. E. Anderson, T. P. Gregory, C. M. McAndrews and L. B. Kool, *Organometallics*, 1990, **9**, 1702.
20 D. Shriver and M. A. Drezdzon, *The Manipulation of Air Sensitive Compounds*, 2nd edn., Wiley, New York, 1986.
21 S. Doniach and M. Sunjic, *J. Phys. Chem.*, 1970, **2**, 285.
22 L. J. van der Pauw, *Philips Res. Rep.*, 1958, **13**, 1.
23 J. A. Riddick, W. B. Bunger and T. K. Sakano, *Organic Solvents*, 4th edn., Interscience-Wiley, New York, 1986.
24 K. M. Kadish and J. E. Anderson, *Pure Appl. Chem.*, 1987, **59**, 5, 707.
25 E. P. Parry and R. A. Osteryoung, *Anal. Chem.*, 1965, **37**, 1634.
26 A. J. Bard and L. R. Faulkner, *Electrochemical Methods, Fundamentals and Applications*, Wiley, New York, 1980.
27 R. S. Nicholson and I. Shain, *Anal. Chem.*, 1964, **36**, 706.
28 K. M. Kadish, L. A. Bottomley and J. S. Cheng, *J. Am. Chem. Soc.*, 1978, **100**, 2731.
29 K. M. Kadish, *Prog. Inorg. Chem.*, 1986, **34**, 435.
30 J.-L. Cornillon, J. E. Anderson, C. Swistak and K. M. Kadish, *J. Am. Chem. Soc.*, 1986, **108**, 7633.
31 V. T. Coombe, G. A. Heath, A. J. MacKenzie and L. J. Yellowlees, *Inorg. Chem.*, 1984, **23**, 3423.
32 P. G. Rasmussen, J. E. Anderson, O. H. Bailey, M. Tamres and J. C. Bayón, *J. Am. Chem. Soc.*, 1985, **107**, 279.
33 K. R. Dunbar, *J. Am. Chem. Soc.*, 1988, **110**, 8247.
34 C.-F. Shu and M. S. Wrighton, *ACS Symp. Ser.*, 1988, **378**, 415.
35 P. Denisevich, H. D. Abruña, C. R. Leidner, T. J. Meyer and R. W. Murray, *Inorg. Chem.*, 1982, **21**, 2153.
36 H. D. Abruña, P. Denisevich, M. Umana, T. J. Meyer and R. W. Murray, *J. Am. Chem. Soc.*, 1981, **103**, 1.
37 K. W. Nebesny, B. L. Maschhoff and N. R. Armstrong, *Anal. Chem.*, 1989, **61**, 469A.
38 M. M. Ahmas and A. E. Underhill, *J. Chem. Soc., Dalton Trans.*, 1982, 1065.

Received 23*rd April* 1991; *Paper* 1/01911B